pH Controlled Permeability of Lipid/Protein Biomimetic Microcapsules

Zhihua An,[†,‡] Helmuth Möhwald,[‡] and Junbai Li*[,†]

International Joint Lab, Key Lab of Colloid and Interface Science, the Center for Molecular Sciences, Institute of Chemistry, Chinese Academy of Sciences, Zhong Guan Cun, Beijing 100080, China, and Max Planck Institute of Colloids and Interfaces, Golm/Potsdam, D-14476, Germany

Received September 5, 2005; Revised Manuscript Received October 28, 2005

The permeability of lipid and protein microcapsules fabricated by alternating adsorption of human serum albumin (HSA) and L-α-dimyristoylphosphatidic acid (DMPA) on a template and subsequent removal of the core is studied as a function of pH value and supplementary layers. The capsules were permeable for macromolecules (FITC-labeled dextran, M_w 40 kDa) at pH < 4.8 and impermeable at pH > 7.4. The assembly of supplementary DMPA bilayers rendered the capsules impermeable for small hydrophilic molecules such as 6-carboxyfluorescein (6-CF). Hence DMPA/HSA capsules can be resealed after fabrication by supplementary layers. This provides the opportunity of applying such biomimetic membrane capsules as drug carriers or model systems to study biological processes at membranes.

Most biological processes, such as molecular recognition, signal transduction, and molecular transport, occur at native cell surfaces. Thus, a variety of cell membrane models have attracted extensive interest in the past decades.[1−4] Lipid bilayers are structurally analogous to the cell membrane, and coating them with proteins may serve as a biomimetic membrane model. A typical example is the natural structure of myelin consisting of alternating layers of phospholipids and of the myelin basic protein, which forms the insulating coating around the nerve axons. Thus lipid/protein capsules should be feasible with low permeability even for small ions mimicking the biological system.[5,6]

With the development of the layer-by-layer (LbL) self-assembly technique, many smart micro- and nanocontainers for storage, transport, and release have been fabricated.[7−9] Polyelectrolyte multilayer capsules have been fabricated as potential drug carriers.[10−14] The permeability of polyelectrolyte microcapsules can be adjusted by controlling the number of layers as well as the conditions of the environment.[15−18] Some defects are formed during the core removal process; thus, coating with a supplementary layer can seal and adjust the permeability.[19] However, there are restrictions on the biocompatibility of polyelectrolyte capsules as drug carriers.[11] As an important extension of shell materials, the preparation of lipid/protein capsules with properties as good as hitherto for synthetic polymers possesses particular advantages. HSA is a globular protein of known crystal structure, which is responsible for the transport of metabolites in the body.[20−22] It is an abundant protein in human blood. Phospholipids are the main component of cell membranes, and DMPA is an ionic representative of these. As a model for biological membranes, complex films of HSA and DMPA will have significant interest due to their unique biological properties. With such a pair of lipid and protein one may consider to incorporate membrane-specific components such as channels and receptors into the capsule's wall for drug release and specific recognition of biomolecules.

We have demonstrated in previous work that HSA and lipid multilayer films can be directly formed on a drug crystal and on particle surfaces based on the LbL technique to fabricate a drug carrier and a hollow microcapsule.[23,24] In the area of drug delivery, there is an important need for tailored carriers in order to control the drug release rate or to target an area. Thus, the investigation of the permeability of such microcarriers is of specific interest. In this paper, the influence of pH on the permeability of DMPA/HSA microcapsules is investigated. Coating by an additional lipid layer after capsule formation has been done in order to investigate the possible sealing of the defects induced by removal of the colloidal template and thus controlling permeability. Such information is very important for the application of lipid and protein microcapsules in controlled drug release.

Materials and Methods

Materials. Human serum albumin (HSA, lyophilized powder protein, approximately 95% by biuret 66 500 Da), L-α-dimyristoylphosphatidic acid (DMPA), FITC-labeled dextran (with different molecular weights), rhodamine 6G, and 6-carboxyfluorescein (6-CF) were purchased from Sigma. Poly(sodium 4-styrenesulfonate) PSS, M_w 70 000, and poly(allylamine hydrochloride) PAH, M_w 70 000, were purchased from Aldrich. PAH was used as received, whereas PSS was dialyzed against Milli-Q water (cutoff 14 000) and lyophilized before use. Positively charged melamine formaldehyde (MF) and negatively charged polystyrene (PS) particles were provided by Microparticles GmbH, Berlin. Manganese carbonate ($MnCO_3$) particles were prepared by a simple mixing method described in the literature.[25,26] The water used in all experiments was prepared in a three-stage Millipore Milli-Q Plus purification system and had a resistivity higher than 18.2 MΩ·cm.

Capsule Preparation. HSA was dissolved in citric acid buffer solutions at pH 3.8 with a concentration of 1 mg/mL. In this case HSA is positively charged since it has an isoelectric point of 4.8. The lipid solution was prepared in the following way: DMPA was dissolved in a mixed solvent (chloroform/methanol = 1:1), then the solvent was evaporated at 30 °C, and the dried film was put under vacuum at least

* Corresponding author. Phone: +86 10 82614087. Fax: +86 10 82612629. E-mail: jbli@iccas.ac.cn.
† Chinese Academy of Sciences.
‡ Max Planck Institute of Colloids and Interfaces.

10.1021/bm050641s CCC: $33.50
Published on Web 01/14/2006

for 3 h. Afterward, a certain amount of Tris−HCl buffer solution (pH 7.4, 10 mM, 100 mM NaCl) was added to a final lipid concentration of 1 mg/mL. Then, the lipid aqueous solution was sonicated for 1 h. Multilayers on MF particles were fabricated as follows: DMPA solution was added to the MF or $MnCO_3$ particle suspension allowing adsorption for 1 h. The suspension was centrifuged, followed by three washing steps with water in order to remove the excess nonadsorbed DMPA in the solution. Then, HSA buffer solution was added to the suspension allowing adsorption for 20 min, and three washing steps with water were carried out before depositing the next DMPA layer. Alternatively, the above steps were repeated until the desired layers were adsorbed. Finally, hollow capsules were obtained by the following step: the coated MF particles were exposed to 0.1 M HCl for 5−10 min, and the membrane filtration technique[27] was applied to wash with Millipore water in order to remove the dissolved MF oligomers from the solution. The coated $MnCO_3$ particles were exposed to 0.1 M HCl for at least 2 h and then washed three times using a membrane filter. $(PAH/PSS)_4$ microcapsules were prepared by the same procedure.

Electrophoretic Mobility Measurement. DMPA/HSA multilayer growth on PS particles was followed by measuring the electrophoretic mobility of the coated particles using a Malvern Zetasizer 4, by taking the average of five measurements at a stationary level. The mobilities (u) were converted into the electrophoretic potential (ζ) using the Smoluchowski relation $\zeta = u\eta/\epsilon$, where η and ϵ are the viscosity and dielectric permeability of the solution, respectively. All measurements were performed in air-equilibrated pure water without electrolyte. Each datum is the average of five measurements. The precision of the measurement is about ±3 mV.

Confocal Laser Scanning Microscopy (CLSM). CLSM images were taken with the Leica TCS NT confocal system (Leica, Germany), equipped with a 100× oil immersion objective with numerical aperture of 1.4. Equal amounts of capsule suspension in water (pH 6) were mixed with 6-CF (0.01 mg/mL), rhodamine 6G (0.02 mg/mL), and FITC-dextran (2 mg/mL) separately. Observations were performed after 5 min. The capsule permeability was quantified by means of fluorescence recovery after photobleaching (FRAP).[28] FITC-labeled dextran (M_w 10 kDa) was used as a fluorescence probe. The bleaching time for all samples was 10 s. The recovery starting point was the first scan after bleaching. Eight to twelve capsules per sample were bleached, and the fluorescence recovery was followed to calculate the permeability. The FRAP measurement was also carried out on $(PAH/PSS)_4$ microcapsules.

Scanning Force Microscopy. SFM images were recorded in air at room temperature using a Nanoscope III Multimode SFM (Digital Instrument Inc., Santa Barbara, CA). The samples were prepared by applying a drop of the capsule solution onto freshly cleaved mica. SFM images were processed by using nanoscope software and image PC software (version beta 2, Scion Corp.).

Circular Dichroism (CD) spectroscopy. CD spectra were recorded by a JASCO J- 715 spectrophotometer at room temperature over a range of 190−260 nm. All measurements in solution were recorded in a 1 mm path length quartz cell. The DMPA/HSA microcapsules were dried on quartz slides and then measured. Each spectrum is the average of eight acquisitions.

Results and Discussion

DMPA/HSA Assembly. The electrostatic interaction is the main force for the multilayer formation in the LbL self-assembly technique. The consecutive assembly of oppositely charged materials onto PS particles should cause a regular reversal of the ζ-potential of the particles from positive to negative or negative to positive. Figure 1a shows the ζ-potential changes after deposition of an HSA layer on negatively charged PS particles in different pH buffer solutions. The concentration of the HSA solution is 1 mg/mL, and the deposition time is 20 min. Several pH values below 4.8 (the isoelectric point of HSA) were chosen for measurement because HSA is positively

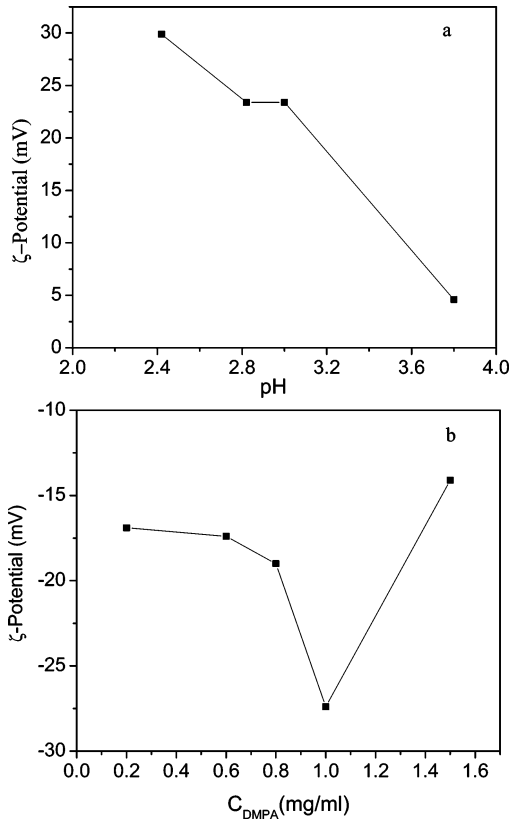

Figure 1. (a) ζ-Potential of an HSA layer deposited on precoated PS particles with HSA at different pH solutions. The concentration of HSA is 1 mg/mL, and the deposition time is 20 min. (b) ζ-Potential of DMPA layer coated HSA/PS particles with different concentrations of DMPA solution. The pH of the HSA solution is 3.8. The concentration of HSA is 1 mg/mL, and the deposition time is 20 min.

charged at those values. The results show that the ζ-potential of the particles was reversed to positive at the selected pH conditions (lower than 4.8). This confirms that the HSA was successfully deposited onto the PS particles. One also notices that the ζ-potential increases with the decrease of pH values of the HSA solution as expected. Finally, pH 3.8 was chosen as a comparatively gentle condition to fabricate the microcapsule.

DMPA was used as a negatively charged component to fabricate DMPA/HSA microcapsules. Figure 1b shows the ζ-potential change after DMPA deposition for different concentrations. The concentration of the HSA solution is 1 mg/mL, and the pH value of the HSA solution is 3.8. The deposition time of the HSA layer is 20 min. The deposition time for the DMPA layer is 1 h. The ζ-potential was definitely reversed to negative by the assembly of DMPA on HSA-coated PS particles. However, one may notice that the decreasing tendency of the ζ-potential with increasing concentration of DMPA was changed when the concentration increased to 1.5 mg/mL. The ζ-potential became higher while increasing the concentration of DMPA. Usually, the adsorption of DMPA on an HSA surface is considered as a spreading of vesicles as described in the literature.[29] The higher concentration of the DMPA vesicle solution may induce an ineffective spreading of DMPA vesicles. On the other hand, the aggregation of the coated colloids became obvious with the increase of the concentration of the DMPA vesicle suspension to 1.5 mg/mL. Thus, we presume that the phospholipids density on the HSA surface increases by increasing the DMPA concentration up to 1 mg/mL, and we use this concentration to obtain capsules with complete lipid bilayer coating. The $(DMPA/HSA)_4$ capsules were stable for more than 3 weeks.

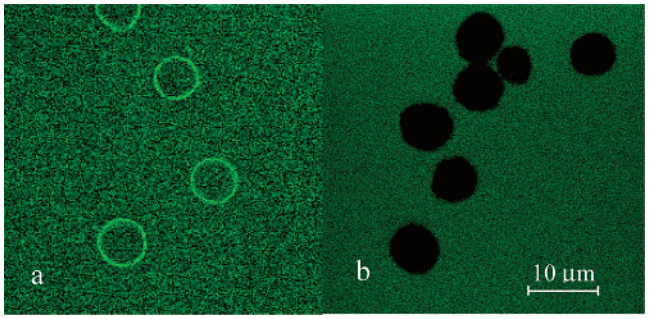

Figure 2. CLSM images of $(DMPA/HSA)_4$ capsules incubated with a fluorescent probe: (a) permeable; (b) impermeable. All observations were performed in water (pH 6).

Table 1. Qualitative Permeability Variation of $(DMPA/HSA)_4$ Hollow Capsules as a Function of the Size of the Fluorescence Probe[a]

fluorescent probe	permeability
dextran 2 000 000	0
dextran 40 000	0
dextran 10 000	100
dextran 4000	100
rhodamine 6G	100
6-CF	100

[a] All measurements were performed in water (pH 6). Note: "0" in the table denotes impermeable and "100" denotes permeable.

Permeability and FRAP Measurement. The permeation of small molecules and macromolecules was followed by CLSM after 5 min of incubation with the fluorescent probe. An equal amount of capsule suspension in water (pH 6) was mixed with different fluorescent molecules. They were considered as permeable when the fluorescence intensity between the interior and outside of the capsule was similar, whereas capsules with dark interiors were considered as impermeable. A typical CLSM image of impermeable and permeable hollow capsules is shown in Figure 2. Rhodamine 6G and 6-carboxyfluorescein (6-CF) were used as small fluorescent dyes. FITC-dextran with different molecular weights was used as a macromolecular probe. The qualitative permeability variation of $(DMPA/HSA)_4$ hollow capsules as a function of the size of the fluorescence probe is given in Table 1. The "0" in the table means that capsules are impermeable, and the "100" means that they are permeable. More than 30 capsules were counted for each data point. The hollow capsules are highly permeable to 6-CF and rhodamine 6G. FITC-dextran with a molecular weight of 10 kDa can also penetrate into the capsules. However, the capsules become impermeable to dextran when a molecular weight higher than 40 kDa was used. This shows that the DMPA/HSA microcapsule is semipermeable. One notices that the permeability of DMPA/HSA microcapsules qualitatively differs for FITC-dextran with molecular weight below 10 kDa and above 40 kDa. This is reasonable considering that dextran with a different molecular weight has a different gyration radius and end-to-end distance. Dextran with a molecular weight of 42 kDa has a gyration radius of 5.8 nm and an end-to-end distance of 13.2 nm. When the molecular weight decreases to 20 kDa, the gyration radius and end-to-end distance of dextran decrease to 4.7 and 6.9 nm, respectively.[30] The threshold behavior of the permeability of the DMPA/HSA capsules as a function of molecular weight indicates that macromolecules with a size less than 5.8 nm can penetrate into the capsules.

The permeability of lipid/protein microcapsules was quantified by means of fluorescence recovery after photobleaching

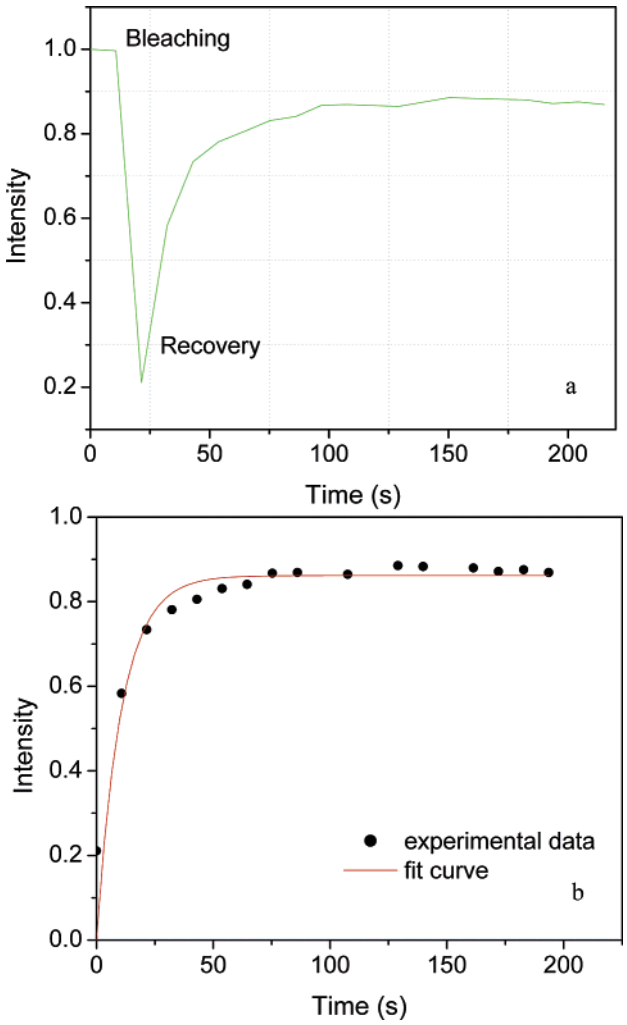

Figure 3. (a) Typical curve of fluorescence bleaching and recovery of $(DMPA/HSA)_4$ capsules. (b) A fit recovery curve using eq 2. FITC-labeled dextran (M_w 10 kDa) was used as a fluorescence probe for FRAP.

(FRAP), as described in the literature.[28] In brief, a laser beam with full intensity bleaches all mobile fluorescein molecules in the capsules, then the fluorescing molecules of the nonbleached area in the bulk begin exchanges into the interior of the capsules. Thus, the fluorescence recovery in the capsule's interior as a function of time is observed at lower excitation intensity. A typical curve of fluorescence bleaching and recovery of $(DMPA/HSA)_4$ capsules is shown in Figure 3a. The recovery curve of the fluorescence intensity $I(t)$ as a function of time t is theoretically described by eq 1:

$$I(t) = I_0 + (I_s - I_0)(1 - e^{-3Pt/r}) \quad (1)$$

where I_s and I_0 represent the fluorescence at $t \rightarrow \infty$ and $t = 0$, respectively. P is the permeability and r the radius of the capsule assumed as a sphere. The recovery curve can be fitted by a function:

$$I = I_{ini}(1 - e^{-At}) \quad (2)$$

The coefficient A is related to the permeability according to the function: $A = 3P/r$. A fit recovery curve using eq 2 is shown in Figure 3b. One may note that the fit is reasonable considering the spread of the data points. Thus, the permeability can be calculated. Eight to 12 capsules of every sample were measured

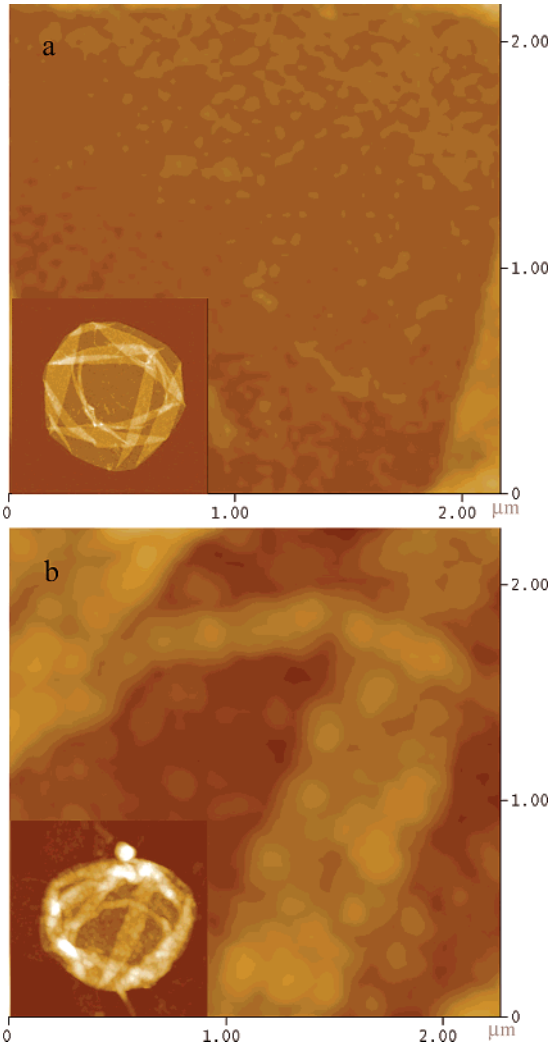

Figure 4. Morphology and roughness of microcapsules measured by AFM: (a) $(DMPA/HSA)_4$; (b) $(PSS/PAH)_4$.

by FRAP using FITC-dextran with a molecular weight of 10 kDa as a fluorescent probe of $(PAH/PSS)_4$ and $(DMPA/HSA)_4$ microcapsules. All values calculated from individual capsules vary by 10%, and the average permeability was finally determined. Comparison with the $(PAH/PSS)_4$ microcapsules (1.1×10^{-7} m/s), which are well-known polyelectrolyte capsules,[17] shows that $(DMPA/HSA)_4$ microcapsules have a lower permeability (7.2×10^{-8} m/s). In fact, the latter has a much higher thickness (104.2 ± 0.5 nm) than the former (16.8 ± 0.5 nm).

Morphology of DMPA/HSA Capsules. The morphology of the dried DMPA/HSA and PSS/PAH capsules was examined by SFM (Figure 4). The result shows that the collapse of DMPA/HSA capsules is similar to the one observed for PSS/PAH capsules due to the evaporation of the aqueous content. Some creases and folds are clearly visible in the inset image of Figure 4, parts a and b. A further magnification of the part of the capsules is shown in Figure 4, parts a and b. It reveals that the surface texture of the DMPA/HSA capsule is much rougher than that of the PSS/PAH capsule. The mean roughness of the capsules was estimated by analyzing a selected area ($1\ \mu m \times 1\ \mu m$) in a fold-free region of each sample as described in the literature.[31] Each data point is the mean value of 6−8 capsules. It reveals that the DMPA/HSA capsules have a higher roughness (6.2 ± 0.2 nm) than the PSS/PAH capsules (2.3 ± 0.3 nm). Such high roughness should be due to the bulkiness of HSA.

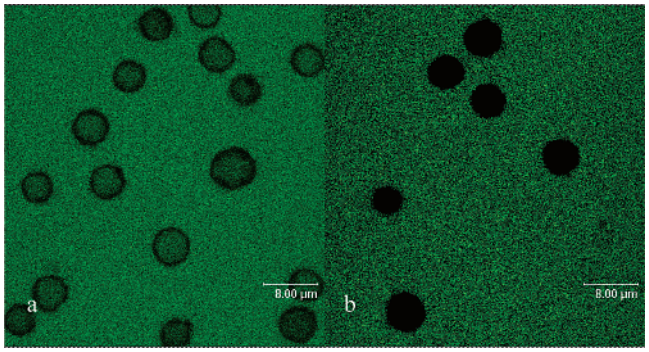

Figure 5. Confocal fluorescence micrograph of $(DMPA/HSA)_4$ microcapsules before (a) and after (b) coating with an additional DMPA layer. 6-CF was used as a fluorescence probe.

The rough structure of the DMPA/HSA multilayer can also explain the higher permeability of the lipid/protein microcapsule compared to that of an intact lipid bilayer with a low permeability that even small polar molecules (6-CF) cannot penetrate.[16,32]

Sealing Capsules with another DMPA Layer. DMPA formed a bilayer structure on the HSA surface as the multilayer of DMPA/HSA assembled on the particles. This was confirmed in our former work.[24] However, DMPA/HSA microcapsules have a higher permeability compared to that of the intact lipid bilayer, which was hypothesized as being due to some channels and holes forming on the capsules' wall during the core removal process. This suggests performing an experiment of coating the hollow capsules with another lipid layer.

$(DMPA/HSA)_4$ hollow microcapsules were coated with one additional DMPA layer in a buffer solution of pH 7.4 (10 mM, 100 mM NaCl); three washing steps with water were proceeded after adsorption for 1 h. 6-CF was used as a small and negatively charged fluorescence probe. Figure 5 shows the CLSM images of DMPA/HSA microcapsules before (a) and after (b) coating with a DMPA layer. 6-CF can penetrate into the DMPA/HSA microcapsules and does not adsorb on the wall due to the same negative charge as the outside layer (Figure 5a). It is obvious that 6-CF cannot penetrate into the microcapsule after the capsules were coated with an additional DMPA layer (Figure 5b). This reveals that the supplemental coating of the capsules with a DMPA layer dramatically changes the permeability of the capsules. This indicates that the capsules were sealed by the DMPA bilayer, which is not permeable for charged species as a consequence of its low dielectric constant.[32] This is a very important observation for the application of biomaterial microcapsules as drug carriers.

pH Effect on Permeability. The permeability of hollow $(DMPA/HSA)_4$ capsules templated on $MnCO_3$ particles for FITC-dextran (M_w 40 kDa) has been studied as a function of pH (Figure 6). The $(DMPA/HSA)_4$ hollow capsules in different pH solutions have been incubated with FITC-dextran (M_w 40 kDa) for 30 min before the measurement. The fluorescence profile along the line indicated in the confocal images shows that the florescence intensity of the interior and exterior of the capsules has no difference when the pH value is lower than 4.8. This is called an "open" state, which means the capsules are permeable for the FITC-dextran with a molecular weight 40 kDa. A lower florescence intensity of the interior compared to that of the exterior is observed when the pH is increased to 6.4. The inside of the capsules remains dark, while the background is fluorescent at pH 7.4. One observes that the capsules "close" for a pH of 7.4 and above. Small molecular dye was also used as a fluorescent probe to measure the

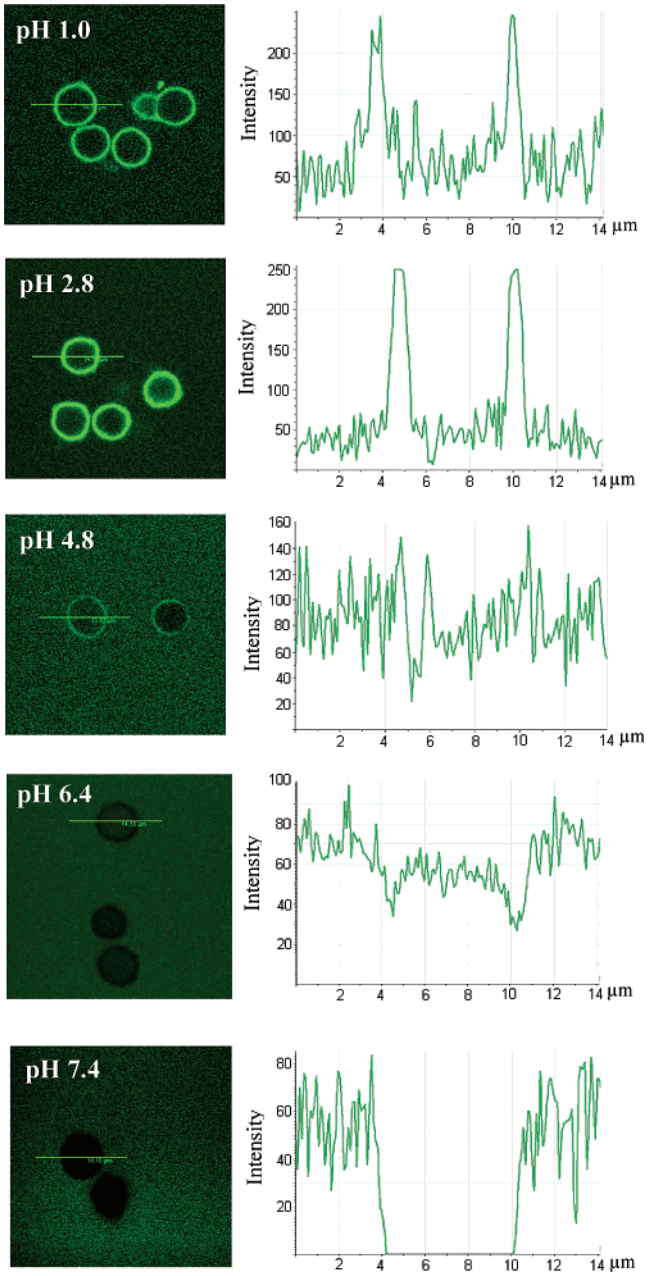

Figure 6. Fluorescence micrographs of $(DMPA/HSA)_4$ capsules in different pH solutions. FITC-dextran (M_w 40 kDa) was used as a fluorescent probe. Left: confocal images of capsules. Right: fluorescence profile along the line indicated in the confocal images.

permeability of hollow capsules; no difference was observed while changing the pH.

The above results indicate that the permeability of lipid/protein microcapsules can be adjusted by changing the pH value of the media. This is reasonable considering the composite of the lipid/protein microcapsule. HSA is stabilized by 17 disulfide bridges and contains a single free sulfydryl.[20,21] The location of the disulfide bridges appears to confer some rigidity within each subdomain, but the lack of interdomain disulfide bridges allows significant modifications in the shape of the HSA in response to changes in pH. The HSA molecule varies in shape between an extended subdomain configuration at low pH 2.5−4.5 and a roughly triangular domain configuration for pH values ranging from 5 to 7.[22] That means the positively charged HSA has maximum opportunities to expose outside to interact with DMPA at the pH 2.5−4.5 region. The order degree of the lipid bilayer structure will decrease when the interaction between the

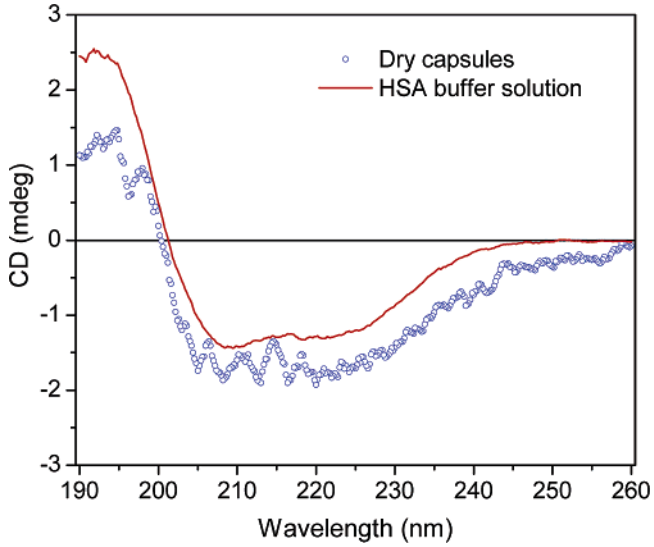

Figure 7. CD spectra of $(DMPA/HSA)_4$ capsules.

lipid and protein increases. A less ordered structure might induce the increase of the permeability. When the pH increases above 5, HSA is negatively charged; therefore, the interaction between HSA and DMPA is mainly repulsive. The order degree of the lipid bilayer structure increases due to the decrease of the interaction of DMPA and HSA. The permeability decreases due to the higher order in the lipid bilayer. In this pH range, the counterions from the coating buffer solution keep the hollow capsules stable. The pH-dependent permeability of the lipid/protein capsules is a cooperative process between the changes of the HSA shape and the changes of the charge of HSA and DMPA. The former changes may induce changes of the spatial conformation of the DMPA/HSA multilayer, while the latter changes may affect the interaction between DMPA and HSA.

One also observes that the florescent molecules can adsorb on the capsules' wall for a pH value equal to or lower than 4.8, while it cannot adsorb on the capsules' wall for a pH value higher than 6.4. This is due to the fact that the positive charge of the HSA outside layer of the $(DMPA/HSA)_4$ capsule increases with the decrease of the pH value. This is consistent with the electrophoretic mobility measurement. As we know, FITC-dextran is slightly negatively charged. The fluorescent molecules are not electrostatically attracted by the capsule's wall for a pH up to 6.4 due to the repulsive force between the same charge of the outside layer HSA and the fluorescence dye.

Secondary Structure of HSA. In our previous work,[24] the secondary structure of HSA at different pH values, which was used to fabricate DMPA/HSA microcapsules, was investigated by circular dichroism (CD) measurement. It indicated the absence of changes of the secondary structure of HSA in the pH range of the hollow capsule fabrication. In this work, a CD spectrum of the DMPA/HSA multilayer microcapsule was obtained by drying a drop of DMPA/HSA microcapsule solution onto quartz slides. By comparison with the secondary structure of HSA in pH 3.8 buffer solutions, one notes that the typical peaks of the α-helix structure of HSA (two minima at 208 and 222 nm wavelength[21]) appeared on the CD spectra of the dried hollow capsules (Figure 7). This reveals that the HSA on the DMPA/HSA microcapsule's wall conserves its secondary structure.

Conclusion. In conclusion, stable DMPA/HSA microcapsules can be successfully prepared by optimizing the fabrication conditions. DMPA/HSA microcapsules are semipermeable, which means that only molecules with a molecular weight lower

than 40 kDa can penetrate into the capsule. The quite rough morphology (6.2 ± 0.2 nm) of the DMPA/HSA microcapsules compared with that of polyelectrolyte capsules can explain the high permeability of such microcapsules and may be strongly affected by the core removal process. The DMPA/HSA microcapsules also show a pH-dependent permeability. Coating an additional DMPA layer can seal the DMPA/HSA microcapsules. Consequently, the permeability of DMPA/HSA capsules can be controlled by the pH value and by supplementary coating. This promising characteristic gives an exciting prospect on applying such biomimetic microcapsules as drug carriers and controlled release systems. The permeability investigation gives also some clues to the interaction between the lipid and protein during their complex film fabrication. Investigations focusing on the recognition and controlled release are underway.

Acknowledgment. We acknowledge the financial support from the National Nature Science Foundation of China (NNSFC29925307 and NNSFC90206035) as well as the collaborated project of the German Max Planck Society. We thank Anne Heilig for AFM measurements.

References and Notes

(1) Hianik, T.; Passechnik, V. I. *Bilayer Lipid Membranes: Structure and Mechanical Properties*; Kluwer Academic Publishers: Dordrecht, The Netherlands, 1995.
(2) Choi, E. J.; Foster, M. D. *Langmuir* **2002**, *18*, 557.
(3) Stamou, D.; Duschl, C.; Delamarche, E.; Vogel, H. *Angew. Chem., Int. Ed*. **2003**, *42*, 5580.
(4) Falconnet, D.; Koenig, A.; Assi, F.; Textor, M. *Adv. Funct. Mater.* **2004**, *14*, 749.
(5) Lu, G.; Chen, H.; Li, J. B. *Colloids Surf., A* **2003**, *215*, 25.
(6) Li, J. B.; Zhang, Y.; Yan, L. L. *Angew. Chem., Int. Ed.* **2001**, *40*, 891.
(7) Lvov, Y.; Ariga, K.; Ichinose, I.; Kunitake, T. *J. Am. Chem. Soc.* **1995**, *117*, 6117.
(8) Lvov, Y.; Ariga, K.; Ichinose, I.; Kunitake, T. *Chem. Commun.* **1995**, 2313.
(9) Decher, G. *Science* **1997**, *277*, 1232.
(10) Donath, E.; Sukhorukov, G.; Caruso, F.; Davis, S.; Möhwald, H. *Angew. Chem., Int. Ed.* **1998**, *37*, 2201.
(11) Qiu, X.; Leoporatti, S.; Donath, E.; Möhwald, H. *Langmuir* **2001**, *17*, 5375.
(12) Caruso, F.; Caruso, R. A.; Möhwald, H. *Science* **1998**, *282*, 1111.
(13) Dai, Z. F.; Dähne, L.; Möhwald, H. *Angew. Chem., Int. Ed.* **2002**, *41*, 4019.
(14) Peyratout, C. S.; Dähne, L. *Angew. Chem., Int. Ed.* **2004**, *43*, 3762.
(15) Shutava, T.; Prouty, M.; Kommireddy, D.; Lvov, Y. *Macromolecules* **2005**, *38*, 2850.
(16) Ge, L.; Möhwald, H.; Li, J. B. *Chem. Eur. J.* **2003**, *9*, 2589.
(17) Ibarz, G.; Dähne, L.; Donath, E.; Möhwald, H. *Adv. Mater.* **2001**, *13*, 1324.
(18) Sukhorukov, G. B.; Antipov, A. A.; Voigt, A.; Donath, E.; Möhwald, H. *Macromol. Rapid Commun.* **2001**, *22*, 44.
(19) Georgieva, R.; Moya, S.; Donath, E.; Baumler, H. *Langmuir* **2004**, *20*, 1895.
(20) Foster, J. F. *Albumin Structure, Function and Uses*; Rosenoer, V. M., Oratz, M., Rothschild, M. A., Eds.; Pergamon: Oxford, 1977.
(21) He, X. M.; Carter, D. C. *Nature* **1992**, *358*, 209.
(22) Olivieri, J. R.; Craievich, A. F. *Eur. Biophys. J.* **1995**, *24*, 77.
(23) An, Z. H.; Lu, G.; Möhwald, H.; Li, J. B. *Chem. Eur. J.* **2004**, *10*, 5848.
(24) An, Z. H.; Tao, C.; Lu, G.; Möhwald, H.; Zheng, S. P.; Cui, Y.; Li, J. B. *Chem. Mater.* **2005**, *17*, 2514.
(25) Silvano, D.; Krol, S.; Diaspro, A.; Cavalleri, O.; Gliozzi, A. *Microsc. Res. Tech.* **2002**, *59*, 536.
(26) Sukhorukov, G. B.; Shchukin, D. G.; Dong, W. F.; Möhwald, H.; Lulevish, V. V.; Vinogradova, O. I. *Macromol. Chem. Phys.* **2004**, *205*, 530.
(27) Voigt, A.; Lichtenfeld, H.; Sukhorukov, G. B.; Zastrow, H.; Donath, E.; Baumler, H.; Möhwald, H. *Ind. Eng. Chem. Res.* **1999**, *38*, 4037.
(28) Ibarz, G.; Dahne, L.; Donath, E.; Möhwald, H. *Chem. Mater*. **2002**, *14*, 4059.
(29) Moya, S.; Donath, E.; Sukhorukov, G. B.; Auch, M.; Bäumler, H.; Lichtenfeld, H.; Möhwald, H. *Macromolecules* **2000**, *33*, 4538.
(30) Barshtein, G.; Tamir, I.; Yedgar, S. *Eur. Biophy. J.* **1998**, *27*, 177.
(31) Leporatti, S.; Voigt, A.; Mitlohner, R.; Donath, E.; Möhwald, H.; Sukhorukov, G. *Langmuir* **2000**, *16* (9), 4059.
(32) Georgieva, R.; Moya, S.; Reichle, C.; Leporatti, S.; Neu, B.; Baumler, H.; Donath, E.; Möhwald, H. *Langmuir* **2000**, *16*, 7075.

BM050641S